Materials Science and Engineering A 378 (2004) 470–474

www.elsevier.com/locate/msea

Dynamics of shape memory alloys patches

Linxiang Wang*, Roderick V.N. Melnik

MCI, Faculty of Science and Engineering, University of Southern Denmark, Sonderborg DK-6400, Denmark

Received 3 June 2003; received in revised form 11 October 2003

Abstract

A two-dimensional mathematical model is constructed in the present paper, which includes the nonlinear coupling of thermal and mechanical fields. The model is based on a two-dimensional approximation to the dynamics of cubic-to-tetragonal and tetragonal-to-orthorhombic phase transformations in shape memory alloys (SMA). It is shown that the Falk model in the one-dimensional case is a special case of the formulated model. Computational experiments are carried out to analyze thermomechanical wave interactions in a thin long strip by applying the finite volume method, while a laminated microstructure in the patch is simulated by using a genetic algorithm.
Published by Elsevier B.V.

Keywords: Shape memory alloys; Phase transformation; Thermomechanics

1. Introduction

A better understanding of the dynamics of phase transitions in shape memory alloys (SMA) is an important task in many areas of applications. However, even for the one-dimensional case, the analysis of this dynamics is quite involved due to a strongly nonlinear pattern of interaction between mechanical and thermal fields [1].

Many instructive investigations have been carried out to understand the martensitic phase transformations, and provided a firm background for the application development, in particular in the one-dimensional cases where the model for shape memory alloys is usually based on the Landau–Ginzburg free energy function [2–4]. Although various approximations to the free energy function have been proposed in the literature for both one- and multi-dimensional cases [4,5], results obtained with two or three-dimensional models are scarce in the context of SMA.

For a number of practical applications, the understanding of the dynamics of SMA structures with dimensions higher than one is required. In this paper, we propose a two-dimensional model describing square-to-rectangular phase transformations in materials with shape memory effects. Such transformations are known to provide an approximation to cubic-to-tetragonal and tetragonal-to-orthorhombic transformations observed in the general three-dimensional case [6,7]. First, we simulate the laminated microstructure based on the chosen form of the free energy function. Then, we reduce the formulated model to a simplified model, and solve the resulting system numerically applying the finite volume method.

2. The two-dimensional mathematical model for SMA dynamics

Based on conservation laws for linear momentum and energy, the system describing coupled thermomechanical wave interactions for the first-order phase transitions in a three-dimensional SMA structure can be written as follows [5,8]:

$$\rho\frac{\partial^2 u_i}{\partial t^2} = \nabla_x \cdot \boldsymbol{\sigma} + f_i, \qquad \rho\frac{\partial e}{\partial t} - \boldsymbol{\sigma}^{\mathrm{T}} : (\nabla \boldsymbol{v}) + \nabla \cdot \boldsymbol{q} = g, \quad i, j = 1, 2, 3, \tag{1}$$

where ρ is the density of the material, $\boldsymbol{u} = \{u_i\}|_{i=1,2,3}$ is the displacement vector, $\boldsymbol{v}$ is the velocity, $\boldsymbol{\sigma} = \{\sigma_{ij}\}$ is the stress tensor, $\boldsymbol{q}$ is the heat flux, e is the internal energy, $\boldsymbol{f} = (f_1, f_2, f_3)^{\mathrm{T}}$ and g are mechanical and thermal loadings, respectively. Let ϕ be the free energy function of a thermomechanical system described by (1). Then, stress and the internal energy function are connected with ϕ by the following relationships:

$$\boldsymbol{\sigma} = \rho\frac{\partial \phi}{\partial \boldsymbol{\eta}}, \qquad e = \phi - \theta\frac{\partial \phi}{\partial \theta}, \tag{2}$$

* Corresponding author. Tel.: +45-6550-1660; fax: +45-6550-1660.
E-mail address: wanglinxiang@mci.sdu.dk (L. Wang).

0921-5093/$ – see front matter. Published by Elsevier B.V.
doi:10.1016/j.msea.2003.10.340

where θ is the temperature, and the Cauchy–Lagrangian strain tensor $\boldsymbol{\eta}$ is given by its components as follows (with the repeated-index convention used):

$$\eta_{ij}(\boldsymbol{x}, t) = \frac{1}{2}\left(\frac{\partial u_i(\boldsymbol{x}, t)}{\partial x_j} + \frac{\partial u_j(\boldsymbol{x}, t)}{\partial x_i}\right), \tag{3}$$

where $\boldsymbol{x}$ are the coordinates of a material point in the domain of interest. Although in the general case, the strain is nonlinear and in some applications the inelastic strain may not be small, the strain linearisation hypothesis has proved to be plausible in a range of SMA application areas (see, e.g., [2] and references therein).

For the cubic-to-tetragonal and tetragonal-to-orthorhombic transformations observed in the general three-dimensional case, a square-to-rectangular transformation can be used as their two-dimensional approximation [6,7]. It is known that for this kind of transformation the free energy function ϕ can be represented in terms of the Landau free energy function F_{L} [6,7,9,10]

$$\begin{aligned}\phi &= -c_v\theta \ln\theta + \tfrac{1}{2}a_1e_1^2 + \tfrac{1}{2}a_3e_3^2 + F_{\mathrm{L}},\\ F_{\mathrm{L}} &= \tfrac{1}{2}a_2(\theta-\theta_0)e_2^2 - \tfrac{1}{4}a_4e_2^4 + \tfrac{1}{6}a_6e_2^6,\end{aligned} \tag{4}$$

where c_v is the specific heat constant, θ_0 is the martensite transition temperature, a_i, $i = 1, 2, 3, 4, 6$ are the material-specific coefficients, and e_1, e_2, e_3 are dilatational, deviatoric, and shear components of strain, respectively. The latter are defined as follows:

$$e_1 = \frac{\eta_{11}+\eta_{22}}{\sqrt{2}}, \qquad e_2 = \frac{\eta_{11}-\eta_{22}}{\sqrt{2}}, \qquad e_3 = \frac{\eta_{12}+\eta_{21}}{2}. \tag{5}$$

Note that the coupling effects between thermal and mechanical fields are included in the formalism (4)–(5). Note further that it is an expansion in the order parameter e_2 up to six-order, which is necessary for modelling of martensitic transformation in SMA [5,4]. By substituting the free energy function defined by (4)–(5) into model (1)–(3), the following coupled system of equations is obtained:

$$\begin{aligned}\frac{\partial^2 u_1}{\partial t^2} &= \frac{\sqrt{2}}{2}\frac{\partial}{\partial x}(a_1e_1 + a_2(\theta-\theta_0)e_2 - a_4e_2^3 + a_6e_2^5)\\ &\quad + \frac{\partial}{\partial y}\left(\frac{1}{2}a_3e_3\right) + f_1,\\ \frac{\partial^2 u_2}{\partial t^2} &= \frac{\partial}{\partial x}\left(\frac{1}{2}a_3e_3\right) + \frac{\sqrt{2}}{2}\frac{\partial}{\partial y}(a_1e_1 - a_2(\theta-\theta_0)e_2\\ &\quad + e_4e_2^3 - a_6e_2^5) + f_2,\\ c_v\frac{\partial\theta}{\partial t} &= k\left(\frac{\partial^2\theta}{\partial x^2} + \frac{\partial^2\theta}{\partial y^2}\right) + a_2\theta e_2\frac{\partial e_2}{\partial t} + g.\end{aligned} \tag{6}$$

In the next two sections, we report the results of simulations of the two-dimensional laminated microstructure governed by the free energy function chosen according to the formalism (4)–(5). Based on the formulated model, we also analyse the dynamical behavior of a thin long SMA strip under thermal loadings.

3. Laminated microstructures in SMA patches

It is already shown for the square-to-rectangular transformation that a laminated microstructure could be formed, which consists of the two martensite variants, if an adequate boundary condition is enforced [11]. The bulk energy of the SMA patch under consideration can be modelled by

$$W(Y) = \int_{\Omega}\phi(\nabla Y)\,\mathrm{d}A, \tag{7}$$

where Ω is the reference configuration associated with the considered SMA patch, Y is the deformation. Supplied with the temperature (below the transformation temperature), the energy function in Eq. (4) attains its minimum value when the deformation gradient ∇Y takes any of the following values:

$$F_0 = \begin{pmatrix} 1+e_{2m}/\sqrt{2} & 0\\ 0 & 1-e_{2m}/\sqrt{2}\end{pmatrix} \text{ or}$$

$$F_1 = \begin{pmatrix} 1-e_{2m}/\sqrt{2} & 0\\ 0 & 1+e_{2m}/\sqrt{2}\end{pmatrix}, \tag{8}$$

where e_{2m} are the local minima of the Landau free energy function given in Eq. (4). Following the idea similar to that proposed in [11] for the approximation of microstructures, we note that our approximation of the deformations at the boundaries, denoted here by $y(x)$, $x \in \partial\Omega$, should satisfy the following boundary conditions:

$$y(x) = (\lambda F_0 + (1-\lambda)RF_1)x, \quad x \in \partial\Omega, \tag{9}$$

where R is a rotation matrix satisfying the so-called twinning equation [11], and λ is the thickness of layers in the laminated microstructure. Conditions (9) are two-variant boundary conditions (constraints) for the energy that has rank-one connected wells, and hence we limit our consideration to two martensite configurations only as represented by (8). Note also that in our implementation, only the deformation on the four corners of the patch is enforced by Eq. (9) while the four edges are free.

The genetic algorithm is applied to simulate the laminated microstructure [12]. The entire patch is approximated by 40×40 nodes. There are totally 120 chromosomes in each generation. The probability of crossover operation is chosen 0.8 while the probability for mutation operation is chosen 0.04.

The distributions of the displacements u_1 and u_2 in the entire patch are shown in Fig. 1(a) and (b), respectively. These computational results have been obtained

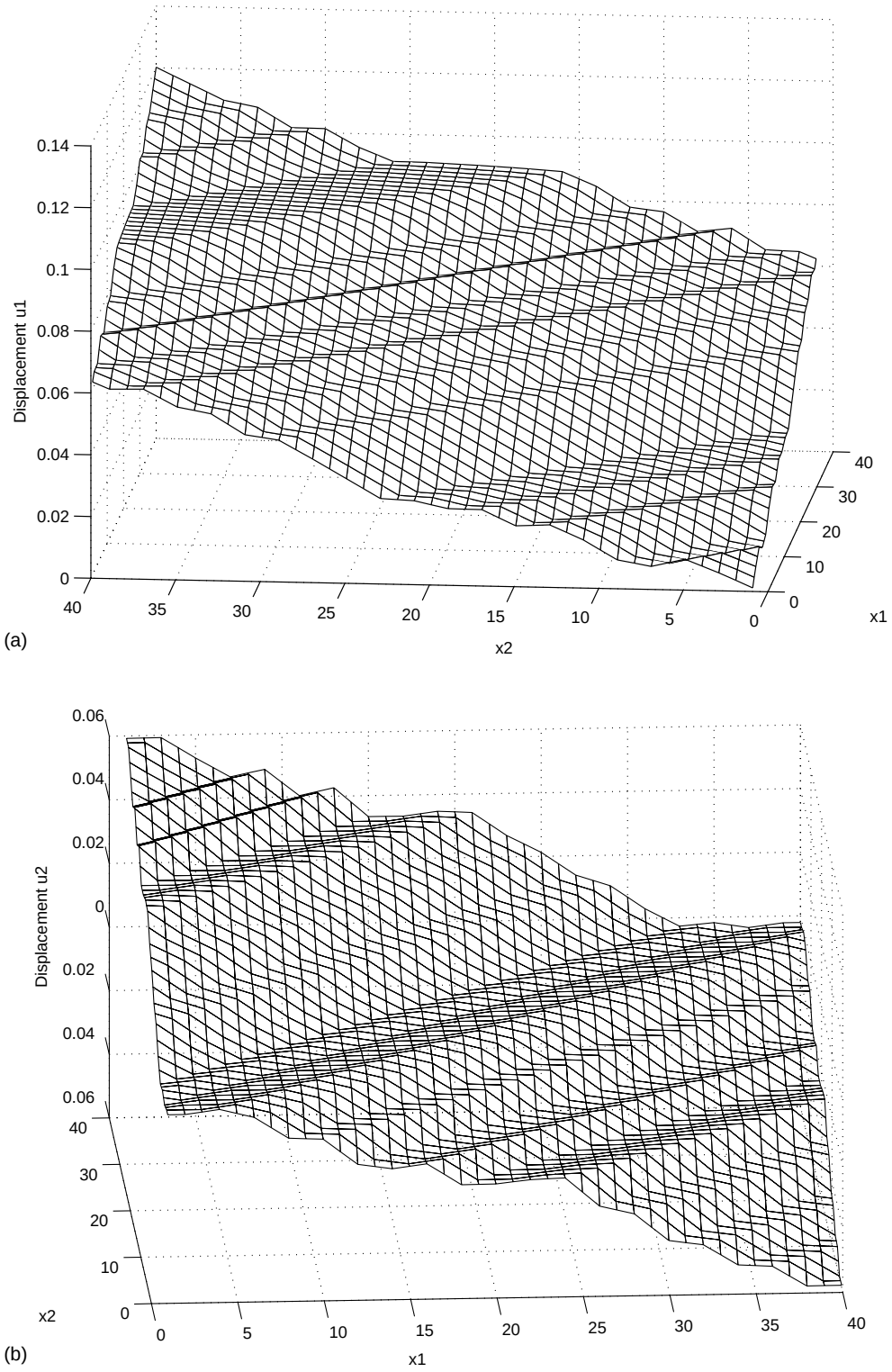

Fig. 1. Simulation results of the laminated microstructure in a SMA patch displacement (a) u_1; (b) u_2.

after the evolution of 30,000 generations. A laminated pattern of the SMA microstructure is well reproduced. No interface energy terms have been included in the current implementation.

4. Dynamics of a SMA strip

When the SMA patch is formed as a thin long strip along one of the directions (e.g., x_1), the deformation of

the two-dimensional SMA structure along that direction will substantially exceed the deformation in the other direction (x_2), so that the deformation along x_2 direction can be neglected. In this case $\partial u_2/\partial x_2 = 0$, $\partial u_2/\partial x_1 = 0$, $\partial u_1/\partial x_2 = 0$, and system (6) is reduced to

$$\rho\frac{\partial^2 u}{\partial t^2} = \frac{\partial}{\partial x}\left(k_1(\theta-\theta_1)\frac{\partial u}{\partial x} - k_2\left(\frac{\partial u}{\partial x}\right)^3 + k_3\left(\frac{\partial u}{\partial x}\right)^5\right) + F,$$
$$c_v\frac{\partial \theta}{\partial t} = k\frac{\partial^2\theta}{\partial x^2} + k_1\theta\frac{\partial u}{\partial x}\frac{\partial^2 u}{\partial x \partial t} + G, \tag{10}$$

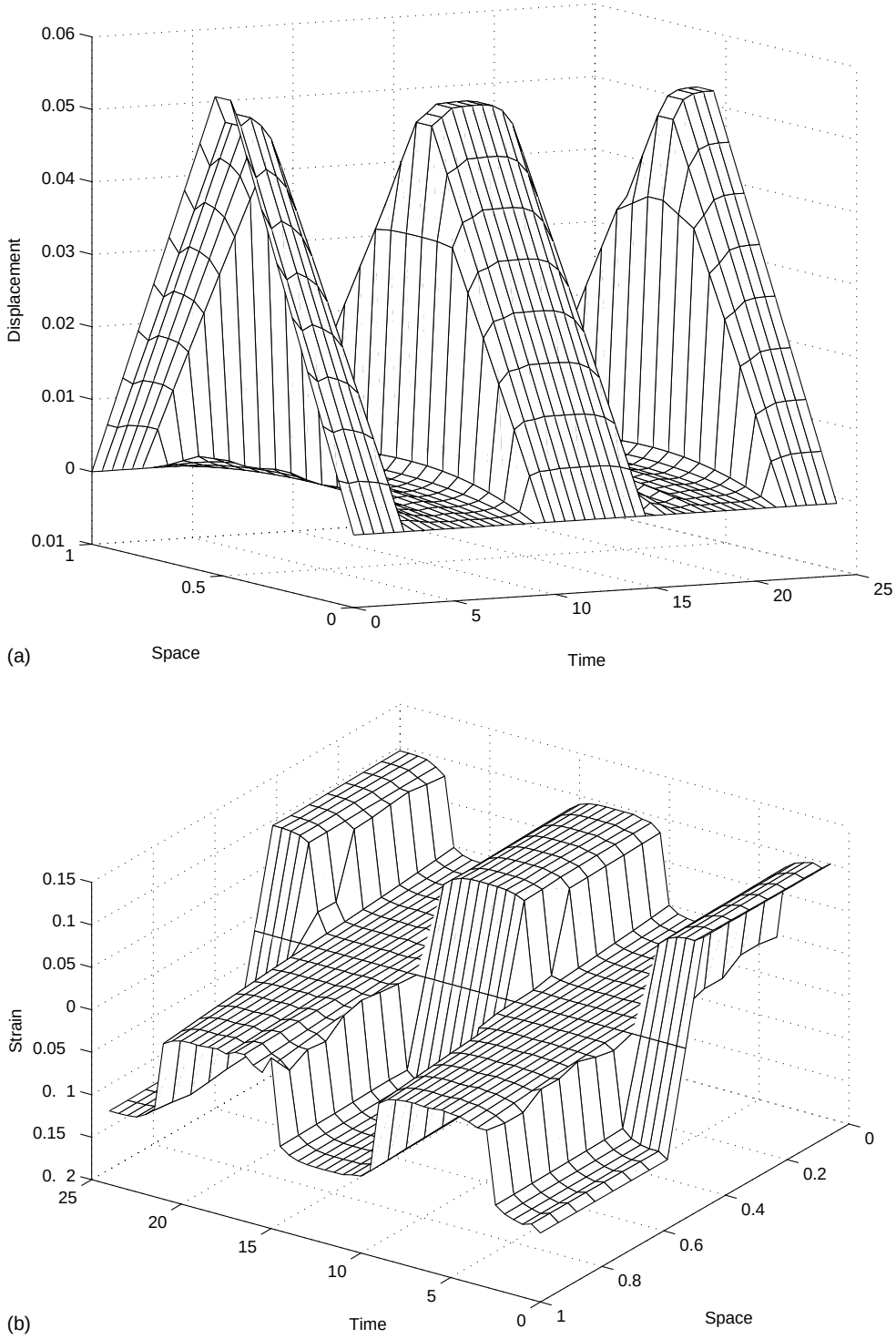

Fig. 2. Numerical results of phase transformation in a SMA strip. Spatio-temporal distribution of (a) displacement; (b) strain.

where k_1, k_2, k_3, c_v and k are re-normalised material-specific constants, and F and G are distributed mechanical and thermal loadings.

For the numerical analysis, it is convenient to introduce two new variables, and re-write system (10) as follows:

$$\begin{aligned} &\frac{\partial u}{\partial t} = v, \qquad \rho\frac{\partial v}{\partial t} = \frac{\partial s}{\partial x} + F, \\ &s = k_1(\theta - \theta_1)\frac{\partial u}{\partial x} - k_2\left(\frac{\partial u}{\partial x}\right)^3 + k_3\left(\frac{\partial u}{\partial x}\right)^5, \\ &c_v\frac{\partial \theta}{\partial t} = k\frac{\partial^2\theta}{\partial x^2} + k_1\theta\frac{\partial u}{\partial x}\frac{\partial v}{\partial x} + G, \end{aligned} \tag{11}$$

where v is the velocity and s is the stress. An efficient methodology based on a reduction of (10) to a system of differential-algebraic equations, has been proposed in [2]. We combine that methodology with the finite volume technique applied to system (11) on a staggered grid. The final solution to the problem is obtained with backward differentiation formula. Since we have to deal with a strong (cubic and quintic) nonlinearities, we have employed a smoothing procedure similar to that proposed in [13]. In particular, we have used the following expansions:

$$\epsilon^3 = \frac{1}{4}\sum_{i=0}^{3}\epsilon^i\epsilon_r^{3-i}, \qquad \epsilon^5 = \frac{1}{6}\sum_{i=0}^{5}\epsilon^i\epsilon_r^{6-i}, \tag{12}$$

where ϵ_r is the strain on time level $n-1$ if the current time level is n (here $\epsilon = \partial u/\partial x$).

Finally, we demonstrate the application of the developed methodology to the analysis of phase transformations in a long thin $Au_{23}Cu_{30}Zn_{47}$ strip of length $L = 1$ cm. For this specific SMA sample, all necessary parameters are taken the same as in [2].

As initial conditions for the model (11) we took two symmetric martensites ($\epsilon^0 = \pm 0.11869$ for $0 \le x \le 0.5$ and $0.5 \le x \le 1$, respectively), $v^0 = 0$, and $\theta^0 = 220$. The distributed mechanical loading was assumed constant as $F = 500\,\mathrm{g/(ms^2\,cm^2)}$, and the distributed thermal loading was assumed as $G = 375\pi\ \sin^3(\pi t/6)\,\mathrm{g/(ms^3\,cm)}$. The boundary conditions for this experiment were taken as pinned-end mechanically and insulated thermally. There were 18 nodes used for u and v in the computational domain (17 nodes were used for s and θ approximated at flux points). Time span of the simulation was [0, 24] (two loading periods) and time stepsize was set to 0.00025. Displacement and strain distributions in the SMA strip are presented in Fig. 2(a) and (b), respectively. The phase transformations are well reproduced by this numerical experiment. Moreover, the temperature-driven phase transformations between martensites and austenite are in quantitative agreement with the results reported in [2].

References

[1] V. Birman, Appl. Mech. Rev. 50 (1997) 629–645.
[2] R.V.N. Melnik, A.J. Roberts, K.A. Thomas, Comput. Mech. 29 (1) (2002) 16–26.
[3] N. Bunber, Continuum Mech. Thermodyn. 8 (1996) 293–308.
[4] F. Falk, P. Konopka, J. Phys. Condens. Matter 2 (1990) 61–77.
[5] I. Pawlow, Control Cybernetics 29 (2000) 341–365.
[6] T. Ichitsubo, K. Tanaka, M. Koiva, Y. Yamazaki, Phys. Rev. B 62 (9) (2000) 5435–5441.
[7] A.E. Jacobs, Phys. Rev. B 61 (10) (2000) 6587–6595.
[8] R.V.N. Melnik, A.J. Robert, K.A. Thomas, Comput. Mater. Sci. 18 (2000) 255–268.
[9] A. Saxena, A.R. Bishop, S.R. Shenoy, T. Lookman, Comput. Mater. Sci. 10 (1998) 16–21.
[10] S. Kartha, Phys. Rev. B 52 (2) (1995) 803–823.
[11] M. Luskin, Acta Numerica 5 (1996) 191–256.
[12] M. Gen, R.W. Cheng, Genetic Algorithm and Engineering Design, Wiley, New York, 1997, p. 64.
[13] M. Niezgodka, J. Sprekels, Numerische Mathematik 58 (1991) 759–778.